Iterative Numerical Computation of the Electromagnetic Fields Inside Weakly Nonlinear Infinite Dielectric Cylinders of Arbitrary Cross Sections Using the Distorted-Wave Born Approximation

Salvatore Caorsi, Andrea Massa, and Matteo Pastorino, *Member, IEEE*

Abstract—**The electromagnetic scattering by weakly nonlinear infinite dielectric cylinders is the topic dealt with in this paper. The cylinders are assumed to be isotropic, inhomogeneous, and lossless and to have arbitrarily shaped cross sections. A time-periodic illumination of the transverse magnetic type is considered. The nonlinearity is assumed to be expressed by the dependence of the dielectric permittivity on the internal electric field, under the hypothesis that the operator responsible for the nonlinearity does not modify the scalar nature of the dielectric permittivity and produces a time-periodic output. The electromagnetic scattering is then described by an integral equation formulation, and the electromagnetic field distributions inside and outside a scatterer are approximated by an iterative numerical procedure starting with the application of the distorted-wave Born approximation. In a simplified version of the approach, the classic first-order Born approximation is used. The convergence of the approach is discussed in several examples. In the computer simulations concerning cylinders with different cross-section shapes, the effects of the nonlinearity on the field-component fundamental frequency were evaluated for different values of the nonlinear parameters in the case of a Kerr-like nonlinearity and of a uniform incident plane wave. The generation of higher-order harmonics was also considered.**

I. Introduction

ELECTROMAGNETIC wave propagation and scattering in the presence of nonlinear materials has been a topic widely investigated in recent years. We refer the reader to several books (e.g., [1]–[5]) and to some more recent papers cited in this text and to the lists of references provided in these papers. Among the various topics related to nonlinear electromagnetics, this paper deals with the scattering of electromagnetic waves by weakly nonlinear dielectric objects. The problem is addressed here from a numerical point view, assuming the nonlinear scatterers to be infinite dielectric cylinders of arbitrary cross-section shapes and illuminated by time-periodic incident waves of the transverse-magnetic type (according to the Shelkunoff terminology [6]). The cylinder cross sections are assumed to be isotropic, nonmagnetic, lossless, and inhomogeneous, the inhomogeneity due not only to the nonlinearity but also to the inhomogeneous nature of the linear part of the dielectric permittivity [7]. In the past, similar topics have been addressed in several papers. For example, the scattering of an obliquely incident plane wave from a weakly nonlinear anisotropic infinite cylinder was studied in [8] using the perturbation method also adopted in [9] for the nonlinear propagation in a nonlinear-filled waveguide. In [10], the author developed a general approach to solving nonlinear scattering problems, assuming phase-matching conditions. He used Volterra-type integrals [11] also used in many other important papers dealing with nonlinear electromagnetic problems [12], [13]. The scattering by nonlinear dielectric layers and by finite nonlinear films has also been considered. For example, in [14] and [15], the scattering of a transverse-electric wave was discussed. In [16], the authors of the present paper proposed a numerical approach to the computation of the electromagnetic scattering by weakly nonlinear bounded objects in free space; the method was based on an integral equation formalism. This approach was further developed in [17], and in [18] the numerical solution was reduced to a global minimization problem.

If one wants to use Maxwell equations, one of the key points is the description of the nonlinear relations between induction and field vectors. In many practical applications, the polarization has very often been expressed in terms of power series of the field [2]. In several cases, nonlinear materials have been assumed to be characterized by a Kerr-like nonlinearity [19] in which the dielectric permittivity was a function dependent on the instantaneous value of the local electric field intensity [7], [14], [15]. Higher-order nonlinearities have been considered in some works. In [16] and [17], a weak nonlinearity was assumed to be expressed by the dielectric permittivity as a function of the internal field under the hypotheses that the medium was isotropic and that the operator was responsible for the nonlinearity being such as to provide a time-periodic output. Such nonlinearity includes, as particular cases, the Kerr-like nonlinearity and higher-order ones [20].

Manuscript received April 9, 1995; revised November 27, 1995.

S. Caorsi is with the Department of Electronics, University of Pavia, 209, I-27100 Pavia, Italy

A. Massa and M. Pastorino are with the Department of Biophysical and Electronic Engineering, University of Genoa, I-16145 Genova, Italy

Publisher Item Identifier S 0018-9480(96)01544-X

In the present paper, on the basis of the integral equation formulation we proposed in [17], we develop an iterative approach for the approximate computation of the fields inside and outside the infinite cylinders considered. The approach is started by using the so-called distorted-wave Born approximation [21], according to which the scattered electric field is expressed in terms of the internal field that would be present in a linear scatterer characterized by the dielectric permittivity of the asymptotic part of the actual nonlinear scatterer. A simplified version is also presented in which the starting point is the use of the classic first-order Born approximation [22] for which the scattered field is approximated by the known incident field. Iterative approaches based on the first-order Born approximation have been found to provide accurate field predictions in linear cases and for very weak scatterers [23]. First-order approximations have also been used for one-dimensional (1-D) nonlinear scattering problems [24]. As to the proposed approach using the distorted-wave Born approximation, the numerical solution is first obtained by using the Richmond formulation [25], which has proved to be effective in dealing with two-dimensional (2-D) scattering by linear dielectrics but only under transverse-magnetic illumination conditions. In [26], we used a similar approach to computing the bistatic scattering width for weakly nonlinear dielectric objects with circular cross sections, but under the additional strong assumption that higher-order harmonics generation was negligible.

Since the approach is an iterative one, the convergence issue is of fundamental importance. Since in a nonlinear case convergence depends on a larger number of factors in comparison with a linear case (as will be discussed in the following), however, we are currently unable to discuss this issue on a theoretical basis. It was considered only via several numerical simulations. In particular in such simulations, we explored the possibility of predicting the effects of a nonlinearity on the field component at the fundamental frequency, for infinite cylinders with different scattering cross sections and for various geometrical and physical configurations. Moreover, the possibility of taking into account third-order harmonics generation was also evaluated. Finally, the application of an upper bound for the numerical discretization, in the light of the nonlinear problem to be handled, is briefly discussed.

II. Mathematical Formulation

Let us consider an infinite dielectric cylinder of arbitrary cross section, S, with the cylindrical axis parallel to the z axis in a Cartesian system of coordinates. The cylinder is illuminated by a time-periodic transverse-magnetic electromagnetic field, $\mathbf{E}^{\text{inc}}(x,y,z,t) = E_z^{\text{inc}}(x,y,t)\mathbf{z}$, $\mathbf{H}^{\text{inc}}(x,y,z,t) = H_x^{\text{inc}}(x,y,t)\mathbf{x} + H_y^{\text{inc}}(x,y,t)\mathbf{y}$. The propagation medium is assumed to be lossless, homogeneous, and characterized by μ_0 and ε_0. The cross section of the cylinder is isotropic and nonmagnetic ($\mu(\mathbf{r}) = \mu_0$). Inside the object cross section, the following Maxwell equations hold

$$\nabla \times \mathbf{E}(x,y,z,t) + \frac{\delta \mathbf{B}(x,y,z,t)}{\delta t} = 0 \tag{1}$$

$$\nabla \times \mathbf{H}(x,y,z,t) - \frac{\delta \mathbf{D}(x,y,z,t)}{\delta t} = 0. \tag{2}$$

As mentioned in the Section I, general relationships for the constitutive equations $\mathbf{D}(\mathbf{E})$ and $\mathbf{B}(\mathbf{H})$ can be written in terms of Volterra series [11]. In many practical cases, however, a nonlinear dielectric permittivity is heuristically assumed, which is expressed in terms of a power series of the field [2]. In this paper, following the formulation we previously proposed in [17], we assume the dielectric permittivity to be dependent on the internal electric field through the relation

$$\varepsilon_{\text{nl}}(x,y,t) = \varepsilon_0[\varepsilon_1(x,y) + \varepsilon_2\{E(x,y,t)\}] \tag{3}$$

where $\varepsilon_1(x,y)$ is the linear part and $\varepsilon_2\{E(x,y,t)\}$ is an operator (responsible for the (weak) nonlinearity), which does not modify the scalar nature of the dielectric permittivity and produces a time-periodic output, under the aforesaid hypothesis on the illuminating field. To simplify the notation, the subscript z denoting the z Cartesian components of the electric field vector is omitted in this relation, as well as in the following ones. The scatterer cross section is inhomogeneous both due to the nonlinearity and in the limit $E(x,y,t) \to 0$ [7]. The above expression for $\varepsilon_{\text{nl}}(x,y,t)$ includes, as particular cases, many nonlinearities used in practical applications, in particular the Kerr-like nonlinearity, which will be considered in the section on numerical examples.

Under the assumptions previously made in [17], it was shown that after expanding $E_z^{\text{inc}}(x,y,t)$, $E(x,y,t)$, and $\varepsilon_2\{E(x,y,t)\}$ in Fourier series at the fundamental frequency $f_0 = \omega_0/2\pi$, in the case of weak nonlinearities, the following inhomogeneous wave equation holds for each harmonic component,

$$\left[\nabla_t^2 + k_m^2\right]\Phi^{s(m)}(x,y) = -k_m^2(\varepsilon_1(x,y) - 1) \times \Phi^{t(m)}(x,y) - k_m^2\Lambda^{(m)}(x,y) \tag{4}$$

where $k_m^2 = m^2\omega_0^2\varepsilon_0\mu_0$, and $\Phi_z^{s(m)}(x,y)$ is the mth harmonic component of the scattered electric field and is given by $\Phi_z^{s(m)}(x,y) = \Phi_z^{t(m)}(x,y) - \Phi_z^{i(m)}(x,y)$, where $\Phi_z^{t(m)}(x,y)$ and $\Phi_z^{i(m)}(x,y)$ are the mth harmonic components of $E(x,y,t)$ and $E^{\text{inc}}(x,y,t)$. The term $\Lambda^{(m)}(x,y)$ is a coupling term dependent on the field components at the same frequency and at other frequencies; it is given by

$$\Lambda^{(m)}(x,y) = \sum_{p=-\infty}^{\infty}\sum_{q=-\infty}^{\infty} \gamma_{ij}^m \Omega_i(x,y)\Phi^{t(j)}(x,y) \tag{5}$$

where $\gamma_{ij}^m = 1$, if $i + j = m$, and $\gamma_{ij}^m = 0$, otherwise. $\Omega_i(x,y)$ is the ith harmonic component of $\varepsilon_2\{E(x,y,t)\}$. The coupling term $\Lambda^{(m)}(x,y)$ can be rendered explicit once the nonlinear operator has been specified. In the section on numerical results, the expression for $\Lambda^{(m)}(x,y)$ in the case of the Kerr-like nonlinearity will be provided. The wave (4) is the scalar analogous to the vector equation (18) in [17], where the three-dimensional (3-D) problem was reduced to a nonlinear system of algebraic equations to be solved in order to obtain a numerical solution.

In this paper, we aim to reach an iterative approximate solution to (4). Such a solution can be achieved by applying

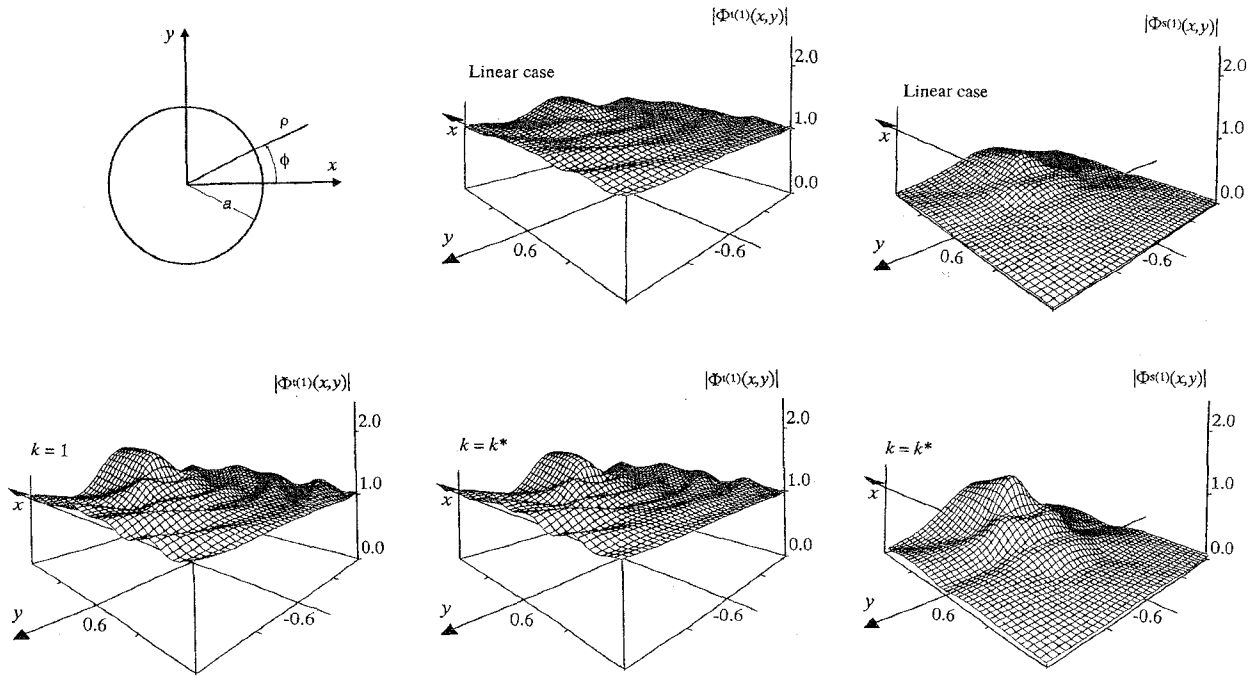

Fig. 1. Scattering by a nonlinear circular cylinder. Amplitudes of $\Phi^{t(1)}(x,y)$ and $\Phi^{s(1)}(x,y)$. ($\Phi_0 = 1$ (V/m), $\phi_0 = 0$, $\varepsilon_1 = 1.3$, $\varepsilon_2 = 0.1$, $k_1 a = 1.5\pi$, $P = 225$).

the so-called distorted-wave Born approximation, which is widely used, especially to solve inverse problems [21]. In particular, we focus on the effects of the nonlinearity on the field components at the fundamental frequency f_0. If we apply the distorted-wave Born approximation, we can express the scattered electric field (for $m = 1$) in terms of the linear internal field, $\Phi^L(x,y)$, i.e., the field that would be present in a cylinder with a homogeneous permittivity equal to the linear part of the actual permittivity. We obtain

$$\Phi^{t(1)}(x,y) = \Phi^{i(1)}(x,y) - j(k_1^2/4)\int_S [\varepsilon_1(x,y)-1]\Phi^L(x',y') \times H_0^{(2)}(k_1\rho)dx'dy' - j(k_1^2/4) \times \int_S \Lambda^{L-(1)}(x',y')H_0^{(2)}(k_1\rho)dx'dy' \quad (6)$$

where $H_0^{(2)}(k_1\rho)$ is the Hankel function of the second kind and the zeroth order and ρ is given by $\rho = [(x-x')^2+(y-y')^2]^{1/2}$ [27]. In (6), the superscript in the term $\Lambda^{L-(1)}(x,y)$ indicates that the coupling term is computed by (5) in terms of the linear field $\Phi^L(x,y)$.

A simpler approximate solution to (5) can be obtained by using the classic first-order Born approximation [22]. In this case, the scattered electric field is expressed in terms of the internal incident electric field. This approximation yields

$$\Phi^{t(1)}(x,y) = \Phi^{i(1)}(x,y) - j(k_1^2/4)\int_S [\varepsilon_1(x,y)-1] \times \Phi^{i(1)}(x',y')H_0^{(2)}(k_1\rho)dx'dy' - j(k_1^2/4) \times \int_S \Lambda^{B-(1)}(x',y')H_0^{(2)}(k_1\rho)dx'dy' \quad (7)$$

where $\Lambda^{B-(1)}(x,y)$ indicates that the coupling term is computed by using (5), on the basis of the incident field only.

In order to develop an iterative process for the computation of the electric field distributions inside and outside S, we assume that the nonlinear field at step $(k+1)$ is given by

$$\Phi_{k+1}^{t(1)}(x,y) = \Phi^{i(1)}(x,y) - j(k_1^2/4)\int_S [\varepsilon_1(x',y')-1] \times \Phi_k^{t(1)}(x',y')H_0^{(2)}(k_1\rho)dx'dy' - j(k_1^2/4) \times \int_S \Lambda_k^{\mathrm{NL}(1)}(x',y')H_0^{(2)}(k_1\rho)dx'dy' \quad (8)$$

where $\Lambda_k^{\mathrm{NL}(1)}(x,y)$ is computed by (6) using $\Phi_k^{t(1)}(x,y)$. Moreover, from (8), it follows that $\Phi_1^{t(1)}(x,y) = \Phi^{i(1)}(x,y)$, if the first-order Born approximation is used, whereas $\Phi_1^{t(1)}(x,y) = \Phi^L(x,y)$, if the distorted-wave Born approximation is applied.

In order to evaluate the convergence of the proposed iterative approach, the following residual error is defined

$$\Re\{k+1\} = S^{-1}\int_S = \left\{\Phi_{k+1}^{t(1)}(x',y') - \Phi^{i(1)}(x',y') + j(k_1^2/4)\right. = S^{-1}\int^S \times \int_S [\varepsilon_1(u,v)-1]\Phi_{k+1}^{t(1)}(u,v)H_0^{(2)} = S^{-1}\int^S \times (k_1\xi)dudv + j(k_1^2/4)\int_S \Lambda_{k+1}^{\mathrm{NL}(1)}(u,v) = S^{-1}\left.\int^S H_0^{(2)}(k_1\xi)dudv\right\}dx'dy' \quad (9)$$

where $\xi = [(x'-u)^2 + (y'-v)^2]^{1/2}$. The approach is assumed to be convergent if $\Re\{k\} \to 0$, as $k \to \infty$. It is

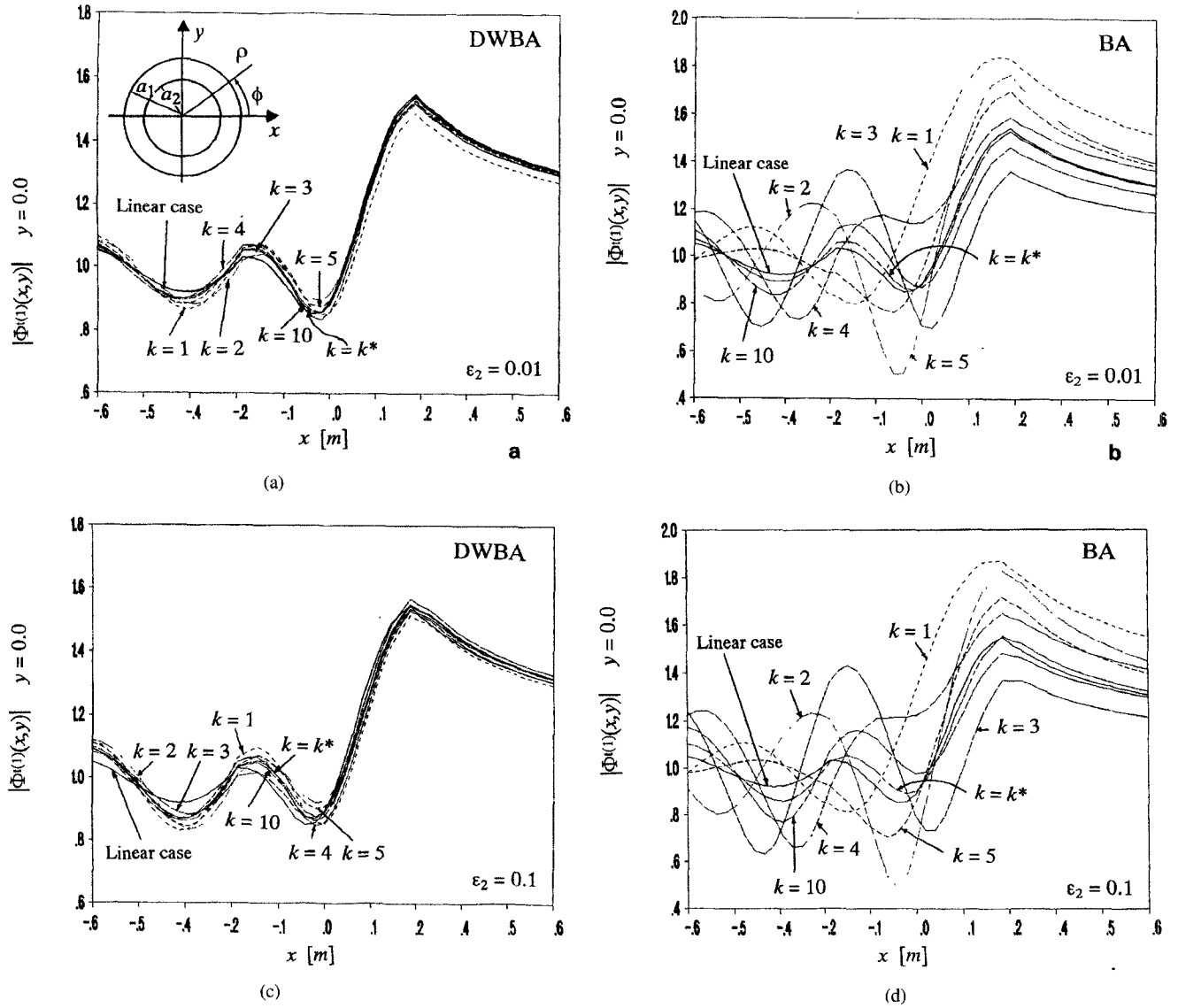

Fig. 2. Scattering by a circular cylinder coated with a nonlinear layer ($\Phi_0 = 1$ (V/m), $\phi_0 = 0$, $\varepsilon_r = 1.8$, $\varepsilon_1 = 1.1$, $k_1 a_2 = 0.49\pi$; $k_1 a_1 = 0.6\pi$, $P = 121$). Comparison between the iterative approaches using the distorted-wave Born approximation (DWBA) and the Born approximation (BA). (a) and (b) $\varepsilon_2 = 0.01$; (c) and (d) $\varepsilon_2 = 0.1$;

well known that, in a linear case, iterative approaches using the Born approximation and the moment method converge if $\max_j\{\lambda_j\} \leq 1$, where λ_j is the jth eigenvalue of the resulting impedance matrix. The above condition can be satisfied for very weakly scattering objects, for which convergence can be explicitly related to the known dielectric parameters of the scatterers. Analogously, in the case of nonlinear scatterers, we can expect the process to be convergent for very weak scatterers only, hence for very weak nonlinearities. Unfortunately, in the present case, convergence depends on various factors: the linear part of the dielectric permittivity, the nonlinear coefficient, and the incident electric field. Unlike linear scattering, for a monochromatic plane wave TM illumination, the amplitude, phase, and frequency values contribute to process convergence or divergence. This makes it impossible to define a criterion that establishes whether convergence can or cannot be reached, given the values of such parameters. Nevertheless, in the Section III, this aspect will be discussed on the basis of several numerical results.

Furthermore, in order to apply the distorted-wave Born approximation, at the first iteration step the field $\Phi_1^{t(1)}(x,y) = \Phi^L(x,y)$ is numerically computed by the Richmond formulation [25], which has been proven to be accurate for forward-scattering by dielectric cylinders if a TM illumination is used [28]. To apply the Richmond method, the cross section S is partitioned into P square subdomains, $p = 1, \ldots, P$. The field and dielectric parameters are assumed to be constant inside each cell, and the problem solution can be obtained by the matrix equation

$$[R]\underline{\Phi}^L = \underline{\Phi}^i \tag{10}$$

where

$\underline{\Phi}^L$ unknown array of dimensions $P \times 1$ whose elements are given by $\phi_p^L = \Phi^L(x_p, y_p)$, $p = 1, \ldots, P$, where (x_p, y_p) is the center of the pth subdomain,

$\underline{\Phi}^i$ excitation array of dimensions $P \times 1$ whose elements are given by $\phi_p^i = \Phi^{i(1)}(x_p, y_p)$, $p = 1, \cdots, P$,

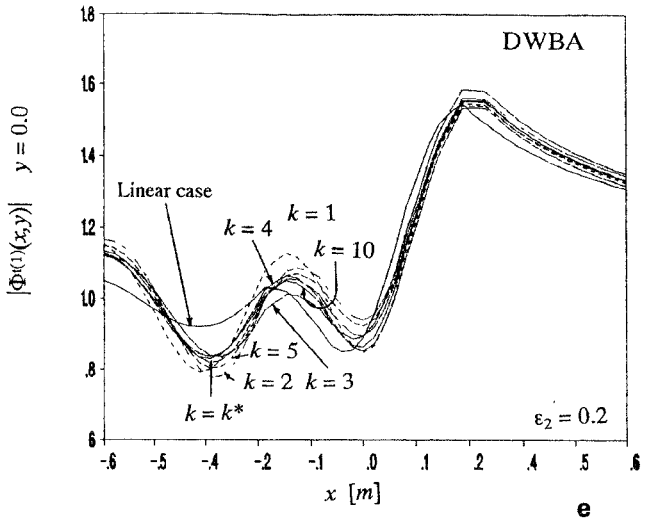

(e)

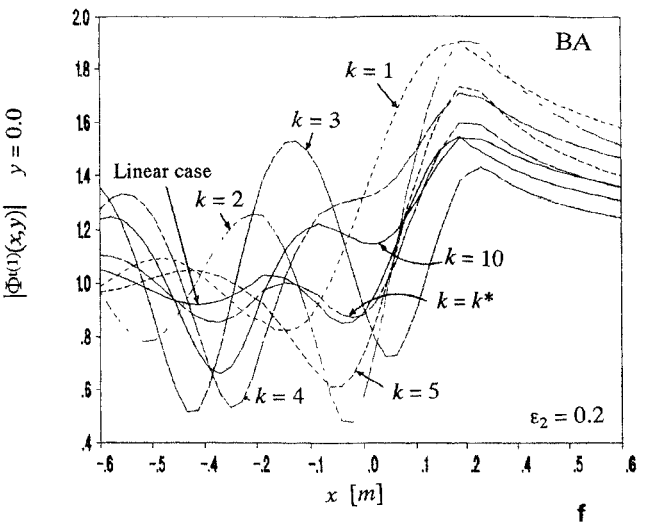

(f)

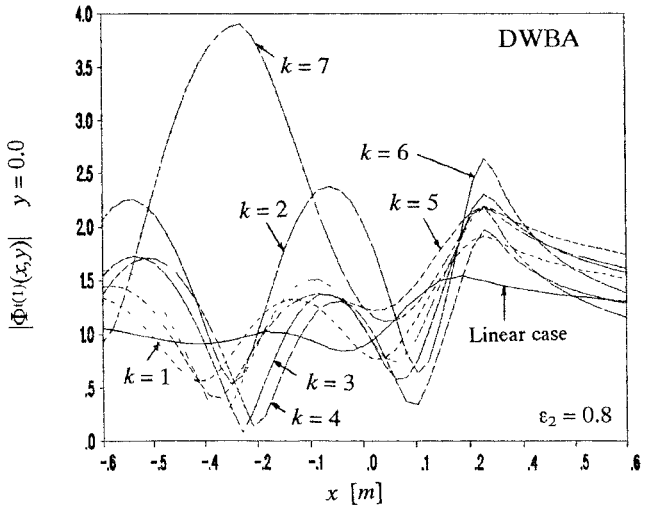

(g)

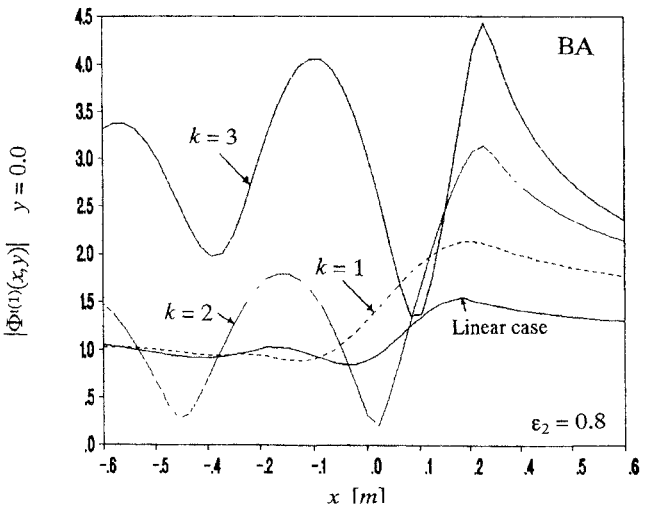

(h)

Fig. 2 Continued. (e) and (f) $\varepsilon_2 = 0.2$, (g) and (h) $\varepsilon_2 = 0.8$

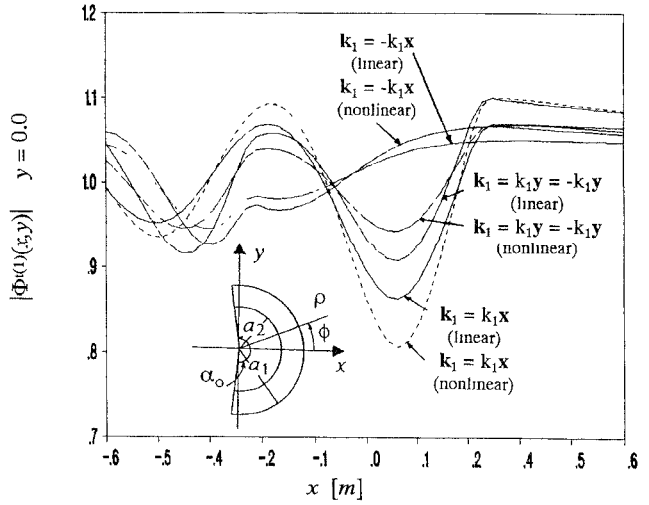

Fig. 3. Scattering by a nonlinear half-shell for different illumination directions. Amplitude of $\Phi^{t(1)}(x, y)$. $\mathbf{k}_1$: propagation vector ($\Phi_0 = 1$ (V/m), $\phi_0 = 0$, $\varepsilon_1 = 1.5$, $\varepsilon_2 = 0.2$, $k_1 a_2 = 0.49\pi$, $k_1 a_1 = 0.6\pi$, $P = 21$, $\alpha_0 = 1.05\pi$, DWBA).

$[R]$ impedance matrix of dimensions $P \times P$ whose generic elements are

$$r_{pq} = (j/2)[\varepsilon_L(x_p, y_p) - 1] \times [\pi k_1 a_p H_1^{(2)}(k_1 \rho_{pq}) - 2j] \quad \text{if } p = q$$

$$r_{pq} = (j/2)[\varepsilon_L(x_p, y_p) - 1] \times \pi k_1 a_p J_1(k_1 b) H_0^{(2)}(k_1 \rho_{pq}) \quad \text{if } p \neq q$$

where $\rho_{pq} = [(x_p - x_q)^2 + (y_p - y_q)^2]^{1/2}$ and $a_p = (S_p/\pi)^{1/2}$, S_p being the area of the pth subdomain.

It is important to note that for linear problems, the discretization should be chosen according to the Hagmann–Gandhi–Durney criterion [29], which relates the maximum linear dimensions of each subdomain to the minimum wavelength of the incident field. In a nonlinear case, the minimum significant wavelength of the field is not known, due to harmonics generation. Therefore, one has to make some *a priori* assumptions in order to fix the maximum linear dimensions of the discretization cells. In this case, the

TABLE I
RESIDUAL ERRORS $\Re\{k\}$ FOR DIFFERENT NUMBERS OF ITERATIONS. SIMULATIONS IN FIG. 2

$k\downarrow$	$\varepsilon_2 = 0.01$		$\varepsilon_2 = 0.1$		$\varepsilon_2 = 0.2$		$\varepsilon_2 = 0.8$	
	DWBA	BA	DWBA	BA	DWBA	BA	DWBA	BA
1	$5.61\cdot10^{-3}$	$4.80\cdot10^{-1}$	$4.88\cdot10^{-3}$	$5.07\cdot10^{-1}$	$7.09\cdot10^{-3}$	$5.37\cdot10^{-1}$	$8.73\cdot10^{-2}$	$7.54\cdot10^{-1}$
2	$2.93\cdot10^{-3}$	$3.04\cdot10^{-1}$	$3.93\cdot10^{-3}$	$3.65\cdot10^{-1}$	$5.79\cdot10^{-3}$	$4.54\cdot10^{-1}$	$1.26\cdot10^{-1}$	$1.92\cdot10^{0}$
3	$1.81\cdot10^{-3}$	$2.09\cdot10^{-1}$	$2.86\cdot10^{-3}$	$2.65\cdot10^{-1}$	$4.49\cdot10^{-3}$	$3.67\cdot10^{-1}$	$1.07\cdot10^{-1}$	$7.07\cdot10^{0}$
4	$1.25\cdot10^{-3}$	$1.50\cdot10^{-1}$	$2.18\cdot10^{-3}$	$2.12\cdot10^{-1}$	$3.67\cdot10^{-3}$	$3.39\cdot10^{-1}$	$8.89\cdot10^{-2}$	$4.66\cdot10^{1}$
5	$8.85\cdot10^{-4}$	$1.08\cdot10^{-1}$	$1.76\cdot10^{-3}$	$1.67\cdot10^{-1}$	$3.37\cdot10^{-3}$	$2.99\cdot10^{-1}$	$1.97\cdot10^{-1}$	$1.90\cdot10^{4}$
6	$6.42\cdot10^{-4}$	$7.76\cdot10^{-2}$	$1.32\cdot10^{-3}$	$1.26\cdot10^{-1}$	$2.70\cdot10^{-3}$	$2.38\cdot10^{-1}$	$2.29\cdot10^{-1}$	$1.79\cdot10^{12}$
:	:	:	:	:	:	:	:	-
12	$9.19\cdot10^{-5}$ ($k^*=12$)	$1.11\cdot10^{-2}$	$3.07\cdot10^{-4}$	$2.98\cdot10^{-2}$	$1.13\cdot10^{-3}$	$1.03\cdot10^{-1}$	$3.44\cdot10^{-1}$	-
:	:	:	:	:	:	:	:	-
13	$< \Re\{k^*\}$	$8.01\cdot10^{-3}$	$2.45\cdot10^{-4}$	$2.31\cdot10^{-2}$	$1.05\cdot10^{-3}$	$9.49\cdot10^{-2}$	$8.08\cdot10^{0}$	-
14	$< \Re\{k^*\}$	$5.81\cdot10^{-3}$	$1.85\cdot10^{-4}$	$1.78\cdot10^{-2}$	$8.54\cdot10^{-4}$	$7.61\cdot10^{-2}$	$4.89\cdot10^{1}$	-
15	$< \Re\{k^*\}$	$4.20\cdot10^{-3}$	$1.50\cdot10^{-4}$	$1.45\cdot10^{-2}$	$7.42\cdot10^{-4}$	$6.82\cdot10^{-2}$	$4.87\cdot10^{3}$	-
16	$< \Re\{k^*\}$	$3.04\cdot10^{-3}$	$1.15\cdot10^{-4}$	$1.09\cdot10^{-2}$	$6.75\cdot10^{-4}$	$6.04\cdot10^{-2}$	$7.57\cdot10^{9}$	
17	$< \Re\{k^*\}$	$2.20\cdot10^{-3}$	$8.92\cdot10^{-5}$ ($k^*=17$)	$1.09\cdot10^{-2}$	$5.42\cdot10^{-4}$	$4.87\cdot10^{-2}$	-	-
:	:	:	:	:	:	:	-	-
27	$< \Re\{k^*\}$	$8.59\ 10^{-5}$ ($k^*=27$)	$< \Re\{k^*\}$	$2.71\ 10^{-4}$	$1.35\ 10^{-4}$	$1.22\ 10^{-2}$	-	-
:	:	:	:	:	:	:	-	-
29	$< \Re\{k^*\}$	$< \Re\{k^*\}$	$< \Re\{k^*\}$	$9.92\ 10^{-5}$ ($k^*=29$)	:	:	-	-
:	:	:	:	:	:	:	-	-
36	$< \Re\{k^*\}$	$< \Re\{k^*\}$	$< \Re\{k^*\}$	$< \Re\{k^*\}$	$8.13\ 10^{-5}$ ($k^*=36$)	$3.31\ 10^{-3}$	-	-
:	:	:	:	:	:	:	-	-
62	$< \Re\{k^*\}$	$< \Re\{k^*\}$	$< \Re\{k^*\}$	$< \Re\{k^*\}$	$< \Re\{k^*\}$	$8.38\ 10^{-5}$ ($k^*=62$)	-	-

Hagmann–Gandhi–Durney criterion for 2-D problems can be expressed as

$$k_M l \leq 2 \tag{11}$$

where $l = a\sqrt{\pi}$ and k_M has been defined in (4), where M is the estimated maximum order of the harmonic components.

Once the approximate linear field $\Phi_1^{t(1)}(x,y) = \Phi^L(x,y)$ has been computed, the iterative process can be implemented by discretizing relation (8) according to the previous scheme

$$\begin{aligned}\Phi_{k+1}^{t(1)}(x,y) \approx \Phi^{i(1)}(x,y) - j\left(k_1^2/4\right)\sum_{p=1}^{P}[\varepsilon_1(x_p,y_p)-1] \\ \times \Phi_k^{t(1)}(x_p,y_p)H_0^{(2)}(k_1\rho_p)\Delta s_p - j\left(k_1^2/4\right) \\ \times \sum_{p=1}^{P}\Lambda_k^{\mathrm{NL}(1)}(x_p,y_p)H_0^{(2)}(k_1\rho_p)\Delta s_p\end{aligned} \tag{12}$$

where $\rho_p = [(x-x_p)^2 + (y-y_p)^2]^{1/2}$. Analogously, the residual error is computed approximately as follows

$$\begin{aligned}\Re\{k+1\} &\approx S^{-1}\sum_{p=1}^{P}\left\{\sum_{p=1}^{P}\Phi_{k+1}^{t(1)}(x_p,y_p) - \Phi^{i(1)}(x_p,y_p)\right\} \\ &= S^{-1}\sum_{p=1}^{P} + j\left(k_1^2/4\right)\sum_{q=1}^{P}[\varepsilon_1(x_q,y_q)-1]\Phi_{k+1}^{t(1)}(x_q,y_q) \\ &= S^{-1}\sum_{p=1}^{P} \times H_0^{(2)}(k_1\xi_{pq})\Delta s_q + j\left(k_1^2/4\right)\sum_{q=1}^{P}\Lambda_{k+1}^{\mathrm{NL}(1)} \\ &= S^{-1}\sum_{p=1}^{P} \times (x_q,y_q)H_0^{(2)}(k_1\xi_{pq})\Delta s_q\Bigg\}\Delta s_p.\end{aligned} \tag{13}$$

Even though in this paper we place emphasis on the effects of the nonlinearity on the fundamental field components, in the following we explore the possibility of predicting the generation of higher-order harmonics. This problem can be faced by using (4) and (5), applied recursively. Let us consider in detail the generation of the third-order harmonic component, under the hypothesis of a monochromatic incident field at a frequency f_0. If we apply the distorted-wave Born approximation, we can express a solution to (4) for $m = 3$ as follows

$$\Phi^{t(3)}(x,y) = -j\left(k_1^2/4\right)\int_S \Lambda^{L-(3)}(x',y')H_0^{(2)}(k_1\rho)dx'dy' \tag{14}$$

where $\Lambda^{L-(3)}(x,y)$ indicates that the coupling term is computed by (5) in terms of the linear field $\Phi^L(x,y)$ (at the

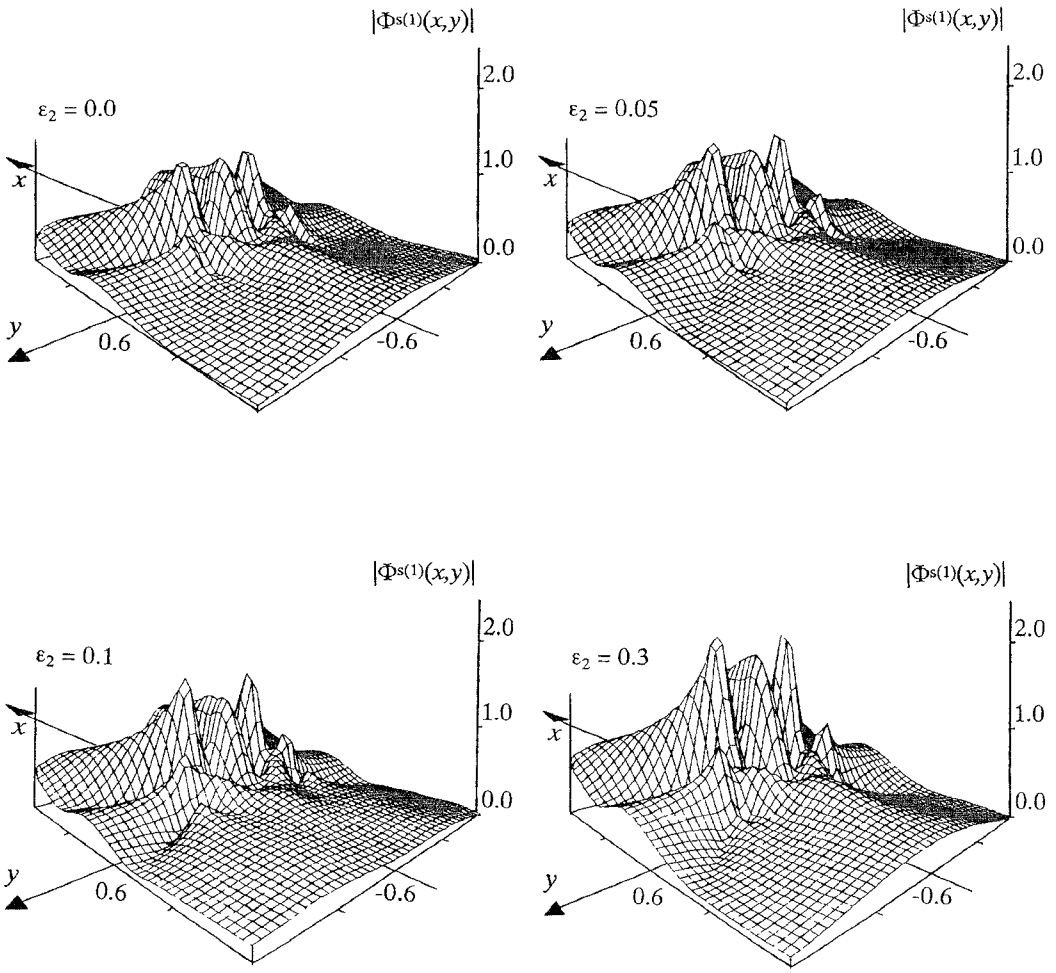

Fig. 4. Scattering by a nonlinear half-shell. Effects of the nonlinear index. Amplitude of $\Phi^{s(1)}(x,y)$. ($\Phi_0 = 1$ (V/m), $\phi_0 = 0$, $\varepsilon_1 = 1.8$, $k_1 a_2 = 0.49\pi$, $k_1 a_1 = 0.6\pi$, $P = 21$, $\alpha_0 = 1.05\pi$, DWBA).

fundamental frequency). If we use the first-order Born approximation, we can replace (14) with

$$\Phi^{t(3)}(x,y) = -j\left(k_3^2/4\right)\int_S \Lambda^{B-(3)}(x',y')H_0^{(2)}(k_3\rho)dx'dy'. \tag{15}$$

At this point, the iterative approach can be expressed by

$$\Phi_{k+1}^{t(3)}(x,y) = -j\left(k_3^2/4\right)\int_S [\varepsilon_1(x',y') - 1]\Phi_k^{t(3)}(x',y') \times H_0^{(2)}(k_3\rho)dx'dy' - j\left(k_3^2/4\right)\int_S \Lambda_k^{\mathrm{NL}(3)}(x',y') \times H_0^{(2)}(k_3\rho)dx'dy' \tag{16}$$

which can be numerically implemented by following the same scheme as previously used for the fundamental field component

$$\Phi_{k+1}^{t(3)}(x,y) \approx -j\left(k_3^2/4\right)\sum_{p=1}^{P}[\varepsilon_1(x_p,y_p) - 1]\Phi_k^{t(3)}(x_p,y_p) \times H_0^{(2)}(k_1\rho_p)\Delta s_p - j\left(k_3^2/4\right) \times \sum_{p=1}^{P}\Lambda_k^{\mathrm{NL}(3)}(x_p,y_p)H_0^{(2)}(k_3\rho_p)\Delta s_p. \tag{17}$$

The same procedure can be applied to derive analogous expressions for all higher-frequency components.

III. Numerical Results

As a first example, we considered the scattering by an infinite cylinder of circular cross section (Fig. 1). The cylinder was illuminated by a TM plane wave given by

$$\Phi^{i(1)}(x,y) = \Phi_0 e^{-j\mathbf{k}_1\cdot\mathbf{u}+\phi_0} \tag{18}$$

where $\mathbf{u} = x\mathbf{x} + y\mathbf{y}$. $|\mathbf{k}_1| = k_1$, and Φ_0 and ϕ_0 are real constants. As mentioned in Section I, the convergence rate depends (unlike the linear case) on Φ_0 and ϕ_0, which are included in the scattering process through (3). The nonlinearity was assumed to be of the Kerr type, for which (3) can be rewritten as

$$\varepsilon_{\mathrm{nl}}(x,y,t) = \varepsilon_0\left[\varepsilon_1(x,y) + \varepsilon_2|E(x,y,t)|^2\right]. \tag{19}$$

As a consequence of this choice, the coefficients $\Omega_i(x,y)$ in (5) can now be rendered explicit. More precisely, they are given by

$$\Omega_i(x,y) = \varepsilon_2 T^{-1}\int_T E(x,y,t)^2 e^{-ji\omega_0 t}dt \tag{20}$$

where $T = 2\pi/\omega_0$.

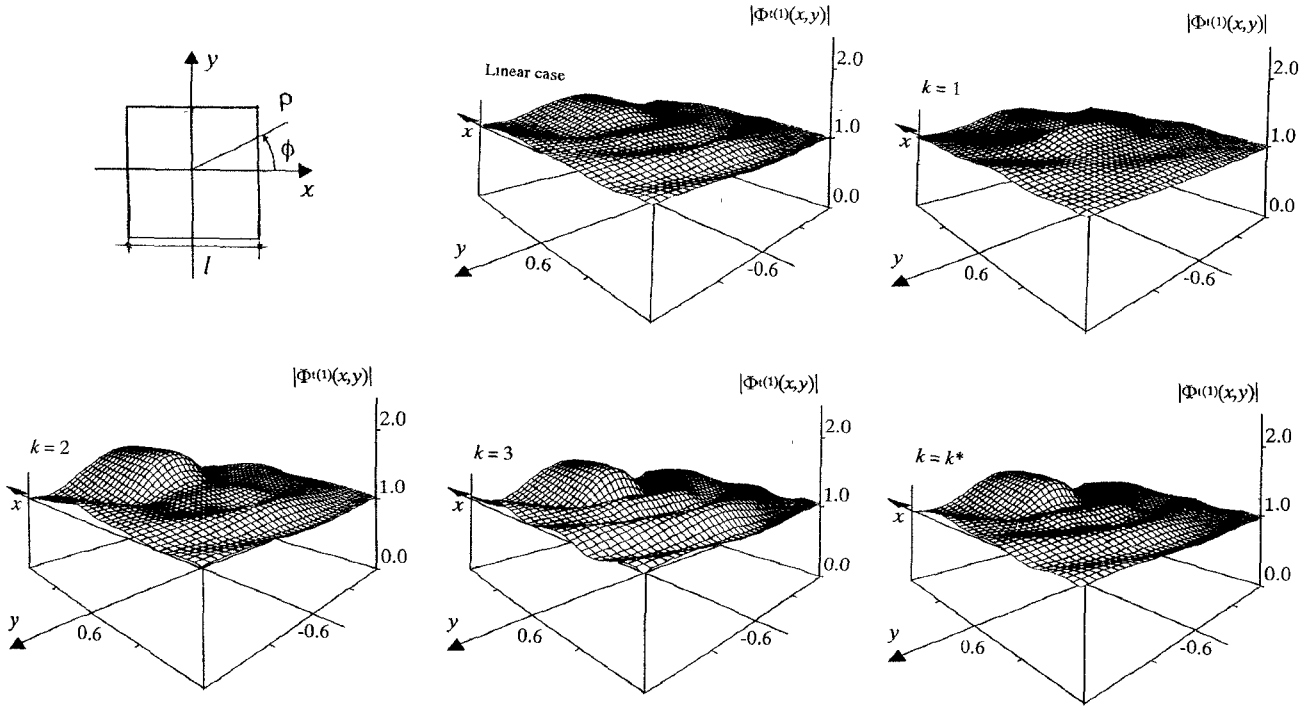

Fig. 5. Scattering by a nonlinear square cylinder. Amplitude of $\Phi^{t(1)}(x, y)$ ($\Phi_0 = 1$ (V/m), $\phi_0 = 0$, $\varepsilon_1 = 1\ 2$, $\varepsilon_2 = 0.08$, $P = 144$, DWBA). $k_1 l = 1.6\pi$

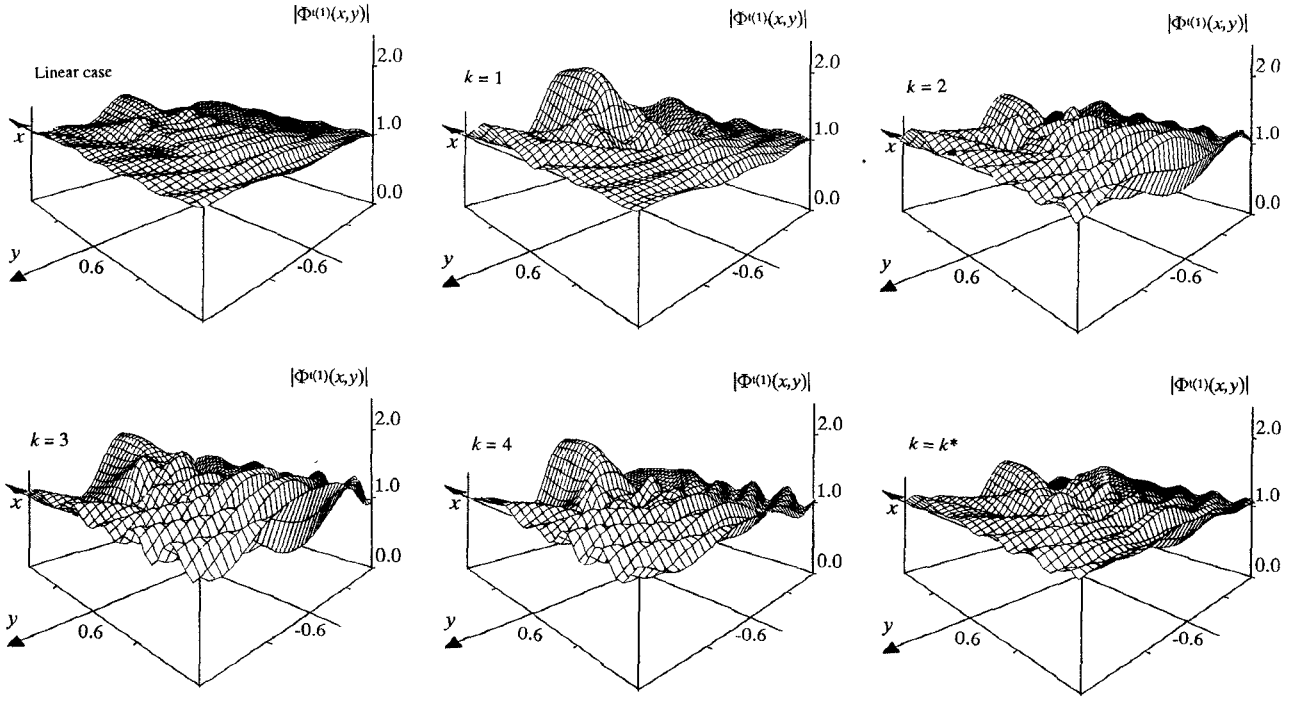

Fig 6. Scattering by a nonlinear square cylinder. Amplitude of $\Phi^{t(1)}(x, y)$ ($\Phi_0 = 1$ (V/m), $\phi_0 = 0$, $\varepsilon_1 = 1.2$, $\varepsilon_2 = 0.08$, $P = 144$, DWBA). $k_1 l = 3.2\pi$.

In this first example, we assumed $\Phi_0 = 1$ (V/m), $\phi_0 = 0$, and $\mathbf{k}_1 = k_1\mathbf{x}$. Moreover, the cross section of the cylinder was assumed to be homogeneous in its linear part ($\varepsilon_1(x, y) = \varepsilon_1 = 1.3$) and with a radius a such that $k_1 a = 1.5\pi$. The other assumed parameters were $\varepsilon_2 = 0.1$ (corresponding to rather a significant nonlinearity) and $P = 225$. Fig. 1 shows pictorial representations of the amplitudes of the total and scattered electric fields (at the fundamental frequency) $\Phi^{t(1)}(x, y)$ and $\Phi^{s(1)}(x, y)$ ($= \Phi^{t(1)}(x, y) - \Phi^{i(1)}(x, y)$), respectively, obtained by using the distorted-wave Born approximation. The figure gives the values for $k = 1$ and the assumed *convergence values*, i.e., the values obtained at a given step k^* at which the residual error $\Re\{k^*\}$ turned out to be less than a fixed threshold value, $\Re_{\text{th}}$. In this case, we assumed $\Re_{\text{th}} = 10^{-4}$. The total and scattered electric fields distributions in the linear case ($\varepsilon_2 = 0.$) are also provided.

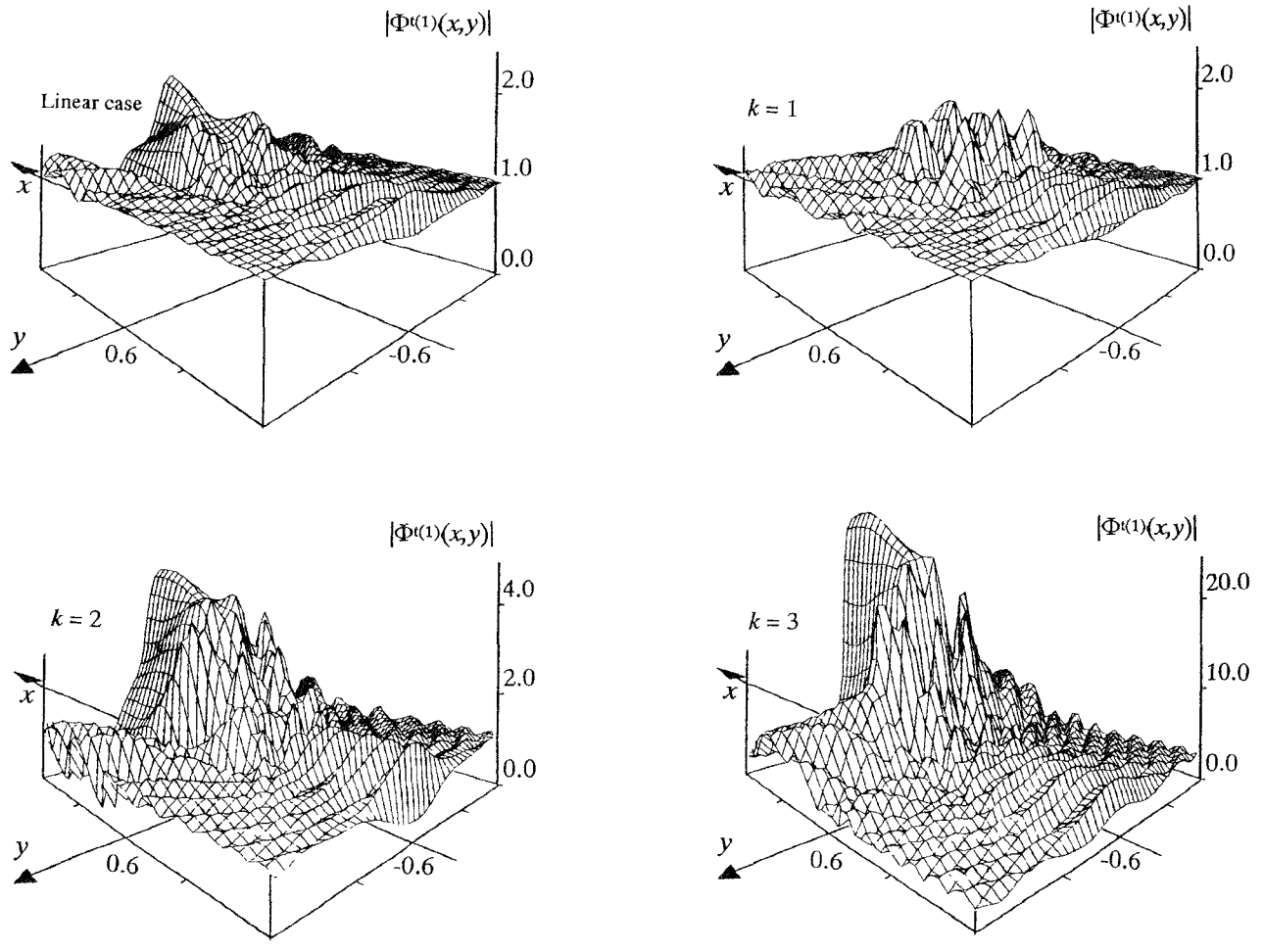

Fig. 7. Scattering by a nonlinear square cylinder. Amplitude of $\Phi^{t(1)}(x, y)$ ($\Phi_0 = 1$ (V/m), $\phi_0 = 0$, $\varepsilon_1 = 1.2$, $\varepsilon_2 = 0.08$, $P = 144$, DWBA). $k_1 l = 6\,4\pi$

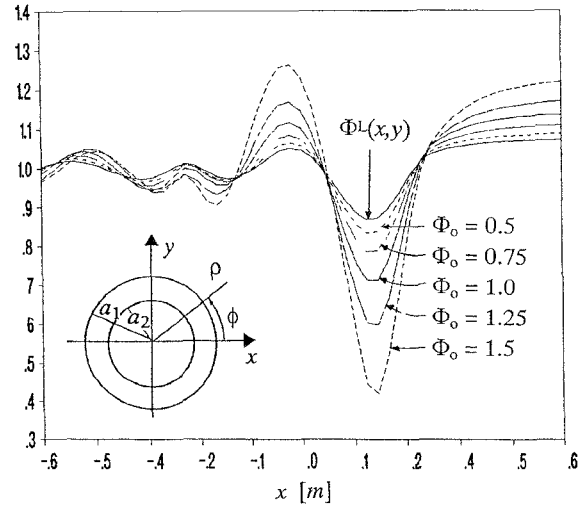

Fig 8. Scattering by a nonlinear shell. Effects of the amplitude of the incident plane wave $\Phi_0(\phi_0 = 0, \varepsilon_1 = 1.2, k_1 a_2 = 0\,49\pi; k_1 a_1 = 0\,6\pi, P = 121$, DWBA)

TABLE II
RESIDUAL ERRORS $\Re\{k\}$ FOR DIFFERENT NUMBERS OF ITERATIONS. SIMULATIONS IN FIG. 4

$k \downarrow$	$\varepsilon_2 = 0.05$	$\varepsilon_2 = 0.1$	$\varepsilon_2 = 0.3$
1	$2.99 \cdot 10^{-4}$	$4.89 \cdot 10^{-3}$	$1.33 \cdot 10^{-1}$
2	$2.95 \cdot 10^{-4}$	$1.21 \cdot 10^{-2}$	$6.27 \cdot 10^{-1}$
3	$3.37 \cdot 10^{-4}$	$9.60 \cdot 10^{-3}$	$4.85 \cdot 10^{0}$
4	$1.17 \cdot 10^{-4}$	$8.00 \cdot 10^{-3}$	$1.90 \cdot 10^{2}$
5	$4.91 \cdot 10^{-5}$ ($k^* = 5$)	$6.63 \cdot 10^{-3}$	$1.79 \cdot 10^{6}$
:	:	:	-
28	$< \Re\{k^*\}$	$9.27 \cdot 10^{-5}$ ($k^* = 28$)	-

A comparison between the approach based on the distorted-wave Born approximation and the version of the approach based on the classic Born approximation was made, considering a homogeneous (linear) dielectric circular cylinder coated with a nonlinear layer (Fig. 2(a)). The incident electric field was given by (18) ($\Phi_0 = 1$ (V/m), $\phi_0 = 0$, and $\mathbf{k}_1 = k_1 \mathbf{x}$) and the other parameters of the two-layer cylinder were ε_r (nucleus) = 1.8, ε_1 (nonlinear layer) = 1.1, $k_1 a_1 = 0.6\pi$, and $k_1 a_2 = 0.49\pi$, $P = 121$. Fig. 2 gives the values of the amplitude of the total electric field, $\Phi^{t(1)}(x, y)$, calculated along the x axis ($y = 0.0$) by using the two algorithms for different values of the nonlinear parameter

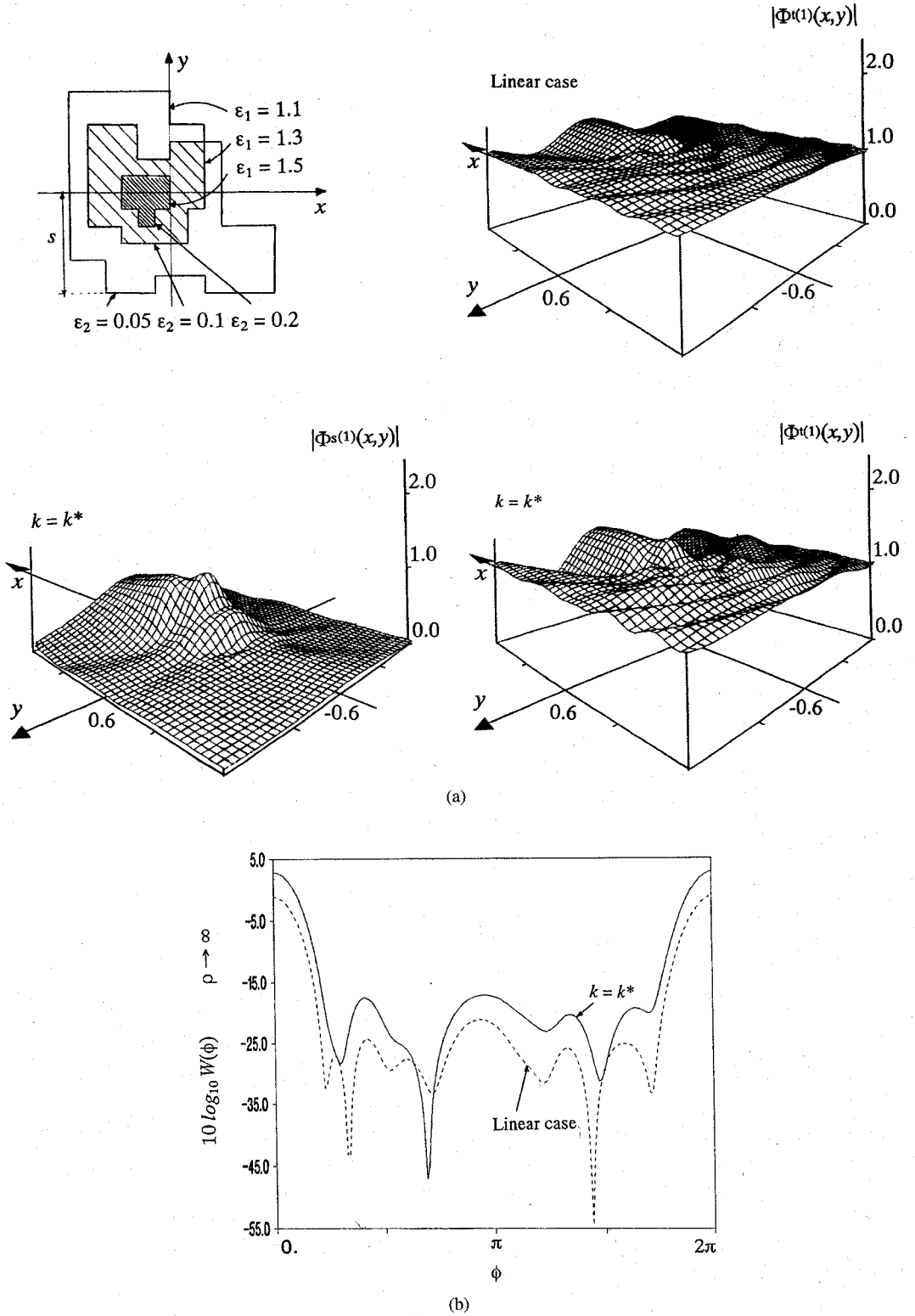

Fig. 9. Scattering by a cylinder of irregular cross section ($\Phi_0 = 1$ (V/m), $\phi_0 = 0$, $\mathbf{k}_1 = k_1\mathbf{x}$, $k_1 s = 1.6\pi$; $P = 106$, DWBA). (a) Amplitudes of $\Phi^{t(1)}(x, y)$ and $\Phi^{s(1)}(x, y)$. (b) Bistatic scattering width ($W(\phi)$).

ε_2. The values obtained in the linear case ($\varepsilon_1 = 0.0$) and analytically computed [30] are also given. In all cases, the process converged quite slowly (even in the linear case), due to the relatively high permittivity of the linear internal cylinder. However, the distorted-wave Born approximation always converged more quickly. For $\varepsilon_2 = 0.8$, the process was divergent, even though the solution at the first iteration may be of some interest. The above considerations are confirmed by the values of the residual error $\Re\{k\}$, which are given in Table I. For this example, we assumed $\Re_{\text{th}} = 10^{-4}$.

In other simulations, a half-shell was considered (Fig. 3). The incident field was assumed to be given by (18), but in

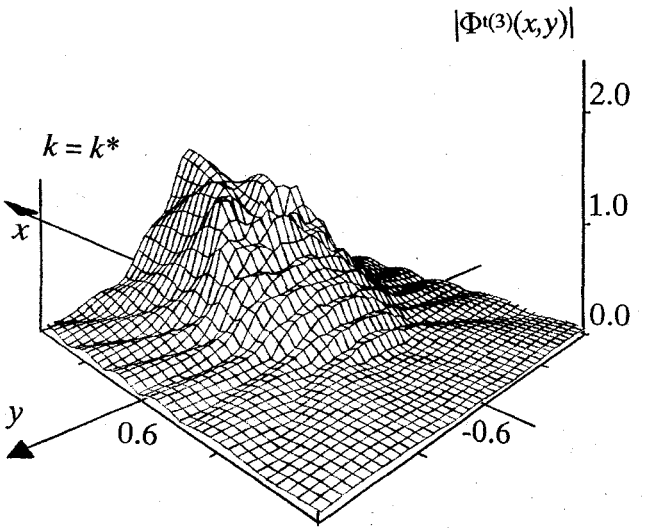

Fig. 10. Scattering by a nonlinear cylinder. Amplitude of $\Phi^{t(3)}(x,y)$ (generated third-order harmonic component). The configuration is the same as in Fig. 1.

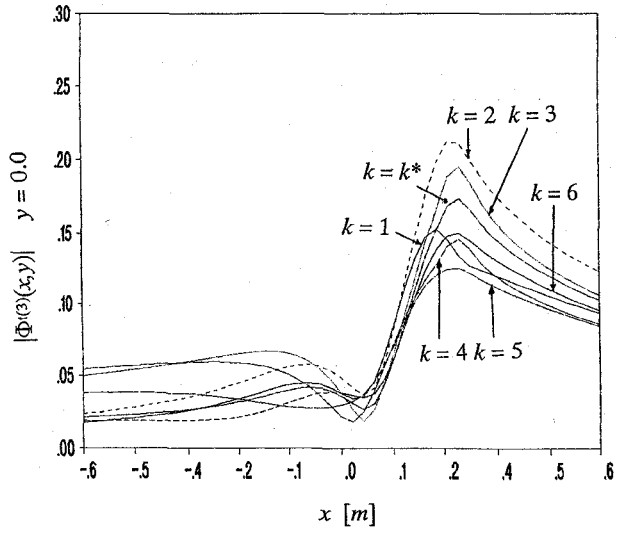

Fig. 11. Scattering by a nonlinear shell. Amplitude of $\Phi^{t(3)}(x,y)$ (generated third-order harmonic component). The configuration is the same as in Fig. 8.

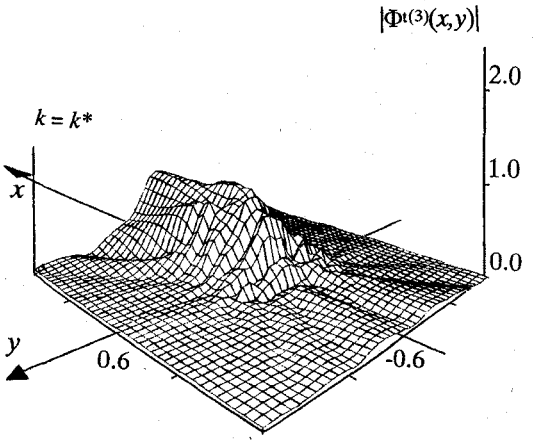

Fig. 12. Scattering by a cylinder of irregular cross section. Amplitude of $\Phi^{t(3)}(x,y)$ (generated third-order harmonic component). The configuration is the same as in Fig. 9.

TABLE III
RESIDUAL ERRORS $\Re\{k\}$ FOR DIFFERENT NUMBERS OF ITERATIONS. SIMULATIONS IN FIGS. 5–7

$k\downarrow$	$k_1 l = 1.6\pi$	$k_1 l = 3.2\pi$	$k_1 l = 6.4\pi$
1	$6.06\cdot10^{-1}$	$8.87\cdot10^{-1}$	$1.50\cdot10^{-1}$
2	$6.75\cdot10^{-2}$	$1.99\cdot10^{-1}$	$2.25\cdot10^{-1}$
3	$2.21\cdot10^{-2}$	$1.95\cdot10^{-1}$	$5.49\cdot10^{-1}$
4	$6.68\cdot10^{-3}$	$1.14\cdot10^{-1}$	$3.34\cdot10^{0}$
5	$1.45\cdot10^{-3}$	$7.15\cdot10^{-2}$	$8.79\cdot10^{2}$
6	$3.45\cdot10^{-4}$	$3.21\cdot10^{-2}$	$2.41\cdot10^{6}$
7	$7.35\cdot10^{-5}$ ($k^*=7$)	$1.95\cdot10^{-2}$	$2.69\cdot10^{19}$
:	:	:	-
18	$<\Re\{k^*\}$	$8.65\cdot10^{-5}$ ($k^*=18$)	-

this case the propagation direction was made to change. In particular, Fig. 3 gives the values of the amplitude of the total electric field $\Phi^{t(1)}(x,y)$, calculated by the distorted-wave Born approximation along the x axis ($y = 0.$) for different values of $\mathbf{k}_1$. In particular, we assumed $\mathbf{k}_1 = k_1\mathbf{x}$, $\mathbf{k}_1 = -k_1\mathbf{x}$, $\mathbf{k}_1 = k_1\mathbf{y}$, and $\mathbf{k}_1 = -k_1\mathbf{y}$. The other assumed parameters were $\Phi_0 = 1$ (V/m), $\phi_0 = 0$, $\varepsilon_1 = 1.5$, $\varepsilon_2 = 0.2$, $k_1 a_2 = 0.49\pi$, $k_1 a_1 = 0.6\pi$, $P = 21$, and $\alpha_0 = 1.05\pi$. The figure also gives the values obtained in the linear case ($\varepsilon_2 = 0.0$). In order to show the effects of the nonlinear index, Fig. 4 gives a pictorial representation of the amplitude of the scattered electric field (at the fundamental frequency) $\Phi^{s(1)}(x,y) = \Phi^{t(1)}(x,y) - \Phi^{i(1)}(x,y)$, computed by using the distorted-wave Born approximation in the $[x,y]$ plane; the scattered field was due to the interaction of the incident field with the same half-shell as in Fig. 3, for $\mathbf{k}_1 = k_1\mathbf{x}$ and $\varepsilon_1 = 1.8$. For $\varepsilon_2 = 0.05$ and $\varepsilon_2 = 0.1$, the figure gives the *convergence values*, whereas for $\varepsilon_2 = 0.3$, the values are those obtained at $k = 1$. The linear values are also given for a comparison, and the values of the residual error $\Re\{k\}$ are given in Table II for a threshold value fixed at $\Re_{\text{th}} = 10^{-4}$.

A cylinder of square section was also considered in order to evaluate the effects of the nonlinearity for different values of the ratio between the wavelength and the linear dimensions of the cross section. Figs. 5–7 show the 3-D representations of the amplitude of the total electric field $\Phi^{t(1)}(x,y)$ in the $[x,y]$ plane at various iteration steps (distorted-wave Born approximation). The assumed parameters were $\Phi_0 = 1$ (V/m), $\phi_0 = 0$, $\mathbf{k}_1 = k_1\mathbf{x}$, $\varepsilon_1 = 1.2$, $\varepsilon_2 = 0.08$, $k_1 l = 1.6\pi$ (Fig. 5), $k_1 l = 3.2\pi$ (Fig. 6), $k_1 l = 6.4\pi$ (Fig. 7), and $P = 144$. The total linear field $\Phi^L(x,y)$ is also plotted. Table III gives the values of the residual error $\Re\{k\}$, for a threshold value fixed at $\Re_{\text{th}} = 10^{-4}$.

The effects of the amplitude of the incident plane wave Φ_0 (which, in linear scattering, plays only the role of a multiplying constant) were considered with reference to a single nonlinear shell (Fig. 8). The shell was characterized by the following geometrical and electrical parameters: $\phi_0 = 0$, $\mathbf{k}_1 = k_1\mathbf{x}$, $\varepsilon_1 = 1.2$, $\varepsilon_2 = 0.2$, $k_1 a_2 = 0.49\pi$, $k_1 a_1 = 0.6\pi$, and

TABLE IV
RESIDUAL ERRORS $\Re\{k\}$ FOR DIFFERENT NUMBERS OF ITERATIONS. SIMULATIONS IN FIG. 9

$k=1$	$k=2$	$k=3$	$k=4$	$k=5$	$k=6$
$2.21\cdot10^{-2}$	$5.31\cdot10^{-3}$	$1.39\cdot10^{-3}$	$3.58\cdot10^{-4}$	$1.22\cdot10^{-4}$	$3.88\cdot10^{-5}$ ($k^*=6$)

$P = 40$. The figure gives the assumed *convergence values* (obtained at step k^*, such that $\Re\{k^*\} \leq \Re_{\text{th}} = 10^{-4}$) of the amplitude of the total electric field $\Phi^{t(1)}(x, y)$ along the x axis ($y = 0$); they were computed by the distorted-wave Born approximation and normalized to Φ_0. The values of the linear field $\Phi^L(x, y)$ (analytically computed and independent of Φ_0) are also provided.

Finally, the scattering by a nonlinear cylinder of irregular cross section and inhomogeneous in its linear part was considered (Fig. 9). We assumed $\Phi_0 = 1$ (V/m), $\phi_0 = 0$, $\mathbf{k}_1 = k_1\mathbf{x}$, $k_1 s = 1.6\pi$, and $P = 106$, $\Re_{\text{th}} = 10^{-4}$. Fig. 9(a) shows the pictorial representations of the total and scattered electric fields at $k = k^*$. Fig. 9(b) gives the bistatic scattering width [31]. Table IV gives the corresponding values of the residual error $\Re\{k\}$.

The prediction of the third-harmonic component generation was considered with reference to the same configuration as shown in Fig. 1. In particular, Fig. 10 gives a pictorial representation of the amplitude of $\Phi^{t(3)}(x, y) = \Phi^{s(3)}(x, y)$, obtained by the iterative scheme defined by (15) and (16) using the distorted-wave Born approximation for $\varepsilon_2 = 0.1$. In the case of a single nonlinear circular shell, i.e., the same as used for the evaluation of the effects of the amplitude of the incident field on the fundamental components, the iterative approach (distorted-wave Born approximation) provided the values of $\Phi^{t(3)}(x, y) = \Phi^{s(3)}(x, y)$ given in Fig. 11. They were computed along the x axis ($y = 0.0$), for $\Phi_0 = 1.25$ and for different numbers of iterations.

Finally, for the irregular scatterer used for the simulation related to Fig. 9, Fig. 12 shows a pictorial representation of the *convergence values* of the amplitude of the third-order harmonic component $\Phi^{t(3)}(x, y)$ obtained at step k^*, at which $\Re\{k^*\} \leq 10^{-4}$ (Table VI).

IV. CONCLUSION

In this paper, an iterative approach to the approximate computation of the fields inside and outside nonlinear cylinders of arbitrary shapes has been described. Starting from the results of an integral-equation formulation for the scattering by bounded weakly nonlinear dielectrics, the approach makes use of the distorted-wave Born approximation; in a simpler version of the approach, the first-order Born approximation is applied. The paper has described the scattering by several cylinders (isotropic, lossless, and nonmagnetic) that had various cross-section shapes and were inhomogeneous in their linear parts. The effects of the nonlinearity, of the linear part of the permittivity, of the amplitude of the incident field, and of the ratio between the wavelength and the linear transversal dimensions on the fundamental harmonic component have been evaluated for Kerr-like nonlinearities. In particular, the convergence of the iterative approach has been discussed. Finally, the generation of the third-order harmonic component has been considered in some examples.

REFERENCES

[1] I. G. Katayev, *Electromagnetic Shock Waves*. London: Iliffe, 1966.
[2] N Bloembergen, *Nonlinear Optics*. New York: Plenum, 1960
[3] G. B. Whitham, *Linear and Nonlinear Waves*. New York: Wiley, 1974.
[4] P. L. E. Uslenghi, Ed., *Nonlinear Electromagnetics*. New York: Academic, 1980.
[5] P. G. Harper and B. S. Whenet, Eds., *Nonlinear Optics*. New York: Academic, 1977.
[6] J. A. Stratton, *Electromagnetic Theory*. New York: McGraw-Hill, 1941.
[7] M. Miyagi and S. Nishida, "Guided waves in bounded nonlinear media (II). Dielectric boundaries," *Sci. Rep. Res. Inst. Tohoku Univ. B (Electron. Commun.)*, vol. 24, pp. 53–67, 1972.
[8] M. A. Hasan and P. L. E. Uslenghi, "Electromagnetic scattering from nonlinear anisotropic cylinders—Part I. Fundamental frequency," *IEEE Trans. Antennas Propagat.*, vol. 38, no. 4, pp. 523–533, Apr. 1990
[9] J. B. Keller and M. H. Millmann, "Perturbation theory of nonlinear wave propagation," *Phys. Rev.*, vol. 181, pp. 1730–1747, 1969.
[10] D. Censor, "Scattering by weakly nonlinear objects," *SIAM J. Appl. Math.*, vol. 43, pp. 1400–1417, 1983.
[11] E. Bedrosian and S. O. Rice, "The output properties of Volterra systems (nonlinear systems with memory) driven by harmonic and Gaussian inputs," *Proc. IEEE*, vol. 59, pp. 1688–1707, 1971.
[12] T. K. Sarkar and D. D. Weiner, "Scattering analysis of nonlinearly loaded antennas," *IEEE Trans. Antennas Propagat.*, vol. AP-24, pp. 125–131, 1976.
[13] D. C. Dalpe, G. Kent, and D. D. Weiner, "Extension of Volterra analysis to weakly nonlinear electromagnetic field problems with applications to Whistler propagation," *IEEE Trans. Microwave Theory Tech.*, vol MTT-30, pp. 1059–1067, 1982.
[14] K. M. Leung, "Scattering of transverse-electric electromagnetic waves with a finite nonlinear film," *J. Opt. Soc. Am. B*, vol. 5, pp. 571–574, 1988.
[15] H.-E. Ponath, U. Trutschel, U. Langbein, and F. Lederer, "Cross trapping of two counterpropagating nonlinear guided waves," *J. Opt. Soc. Am. B*, vol. 5, pp. 539–546, 1988.
[16] S. Caorsi and M. Pastorino, "Integral equation formulation of electromagnetic scattering by nonlinear dielectric objects," *Electromagnetics*, vol. 11, pp. 357–375, 1991.
[17] S. Caorsi, A. Massa, and M. Pastorino, "A numerical approach to full-vector electromagnetic scattering by three-dimensional nonlinear bounded dielectrics," *IEEE Trans. Microwave Theory Tech.*, vol. 43, Feb. 1995.
[18] ——, "Electromagnetic scattering by bounded nonlinear objects by a statistical cooling procedure," in *Proc. Sixth Biennial IEEE Conf Electromagnetic Field Computation*, Aix-les-Bains, France, July 5–7, 1994, p. 323.
[19] L. D. Landau, E. M. Lifsits, and E. Pitaevski, *Electrodynamics of Continuous Media*. Oxford: Pergamon, 1984.
[20] D. Mihalache, D. Mazilu, M. Bertolotti, and C. Sibilla, "Exact solution for nonlinear thin-film guided waves in higher-order nonlinear media," *J. Opt Soc. Am. B*, vol. 5, pp. 565–570, 1988.
[21] R. J. Wombell and R. D. Murch, "The reconstruction of dielectric objects from scattered field data using the distorted-wave Born approximation," *J. Electromagnetic Waves and Applicat.*, vol. 7, pp. 687–702, 1993.
[22] P. M. Morse and H. Feshback, *Methods of Theoretical Physics*. New York: McGraw-Hill, 1953.
[23] R. S. Varga, *Matrix Iterative Analysis*. Englewood Cliffs, NJ: Prentice-Hall, 1962.
[24] F. C. Lin and M. A. Fiddy, "Born-Rytov controversity. II. Applications to nonlinear and stochastic scattering problems in one-dimensional half-space media," *J. Opt. Soc. Am. A*, vol. 10, pp. 1971–1983, 1993
[25] J. H. Richmond, "Scattering by a dielectric cylinder of arbitrary cross-section shape," *IEEE Trans. Antennas Propagat.*, vol. AP-13, pp. 334–341, 1965.

[26] S. Caorsi, A. Massa, and M. Pastorino, "Bistatic scattering width evaluation for nonlinear isotropic infinite circular cylinders," *Microwave and Opt. Technol. Lett.*, vol. 7, pp. 639–642, 1994.
[27] C. T. Tai, *Dyadic Green's Functions in Electromagnetic Theory*. Scanton: International Textbook, 1971.
[28] A. F. Peterson, "Analysis of heterogeneous EM scatterers: Research progress of the past decade," *Proc. IEEE*, vol. 79, pp. 1431–1453, 1991,
[29] M. J. Hagmann, O. P. Gandhi, and C. H. Durney, "Upper bound on cell size for moment-method solutions," *IEEE Trans. Microwave Theory Tech.*, vol. MTT-25, pp. 831–832, 1977.
[30] H. E. Bussey and J. H. Richmond, "Scattering by a lossy dielectric circular cylindrical multilayer numerical values," *IEEE Trans. Antennas Propagat.*, vol. AP-23, pp. 723–725, 1975.
[31] J. A. Balanis, *Advanced Engineering Electromagnetics*. New York: Wiley, 1989.

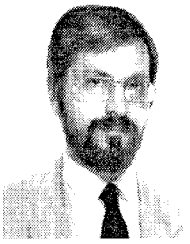

Salvatore Caorsi received the "laurea" degree in electronic engineering from the University of Genoa, Genoa, Italy, in 1973.

After graduation he remained at the university as a Researcher, and since 1976 he has been Associate Professor of Antennas and Propagation at the Department of Biophysical and Electronic Engineering of the University of Genoa. In 1985, he also assumed the title of Professor of Fundamentals of Remote Sensing. Since 1994, he has been Full Professor of Electromagnetic Compatibility at the Department of Electronics of the University of Pavia, Italy. At present, he is responsible for the Inter-University Research Center for Interactions Between Electromagnetic Fields and Biological Systems (ICEMB). His primary activities are focused on applications of electromagnetic fields to telecommunications, artificial vision and remote sensing, biology, and medicine. In particular, he is working on research projects concerning microwave hyperthermia and radiometry in oncological therapy, numerical methods for solving electromagnetic problems, and inverse scattering and microwave imaging.

Dr. Caorsi is a member of the Associazione Elettrotecnica ed Elettronica Italiana (AEI), the European Bioelectromagnetism Association (EBEA), and the European Society for Hyperthermic Oncology (ESHO).

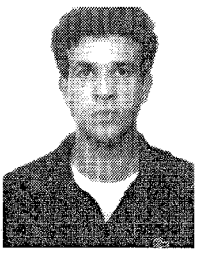

Andrea Massa is a Ph.D. student of electronics and computer science in the Department of Biophysical and Electronic Engineering, University of Genoa, Genoa, Italy. He received the "laurea" degree in electronic engineering from the University of Genoa in 1992.

Since that year, he has cooperated in the activities of the Applied Electromagnetism Group at the University of Genoa. His main interests are in the field of electromagnetic direct and inverse scattering, biomedical applications of electromagnetic fields, nonlinear wave propagation, and numerical methods in electromagnetism.

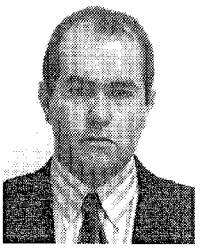

Matteo Pastorino (M'90) received the "laurea" degree in electronic engineering from the University of Genoa, Genoa, Italy, in 1987 and the Ph.D. degree in electronics and computer science from the same university in 1992.

Since 1987 he has been involved in the activities of the Applied Electromagnetics Group and, since its establishment, the Inter-University Research Center for Interactions between Electromagnetic Fields and Biological Systems. At present, he is an Assistant Professor of Electromagnetic Fields in the Department of Biophysical and Electronic Engineering. His main research interests are in electromagnetic direct and inverse scattering, microwave imaging, wave propagation in presence of nonlinear media, and in numerical methods in electromagnetism. He is also working on research projects concerning biomedical applications of electromagnetic fields and microwave hyperthermia.

Dr. Pastorino is a Member of the Associazione Elettrotecnica ed Elettronica Italiana (AEI) and the European Bioelectromagnetism Association (EBEA).